Research Article | Vol. 7, No. 11 | 1 Nov 2017 | OPTICAL MATERIALS EXPRESS 3809
Optical Materials EXPRESS

Detection of phase separation and nano-droplet states in $La_{0.33}Pr_{0.34}Ca_{0.33}MnO_3$ nanowires via near-infrared reflection experiments

HONGYING MEI,[1,2] CHAO ZHANG,[1,2,4] CHAO WANG,[1,2] CHANGNENG LIANG,[3] JIE ZHANG,[3] LAN DING,[3] JIN ZHANG,[3] AND WEN XU[1,3,5]

[1]*Key Laboratory of Materials Physics, Institute of Solid State Physics, Chinese Academy of Sciences, Hefei 230031, China*
[2]*University of Science and Technology of China, Hefei 230026, China*
[3]*School of Physics and Astronomy, International Joint Research Center for Optoelectronic and Energy Materials, and Yunnan Key Laboratory for Micro/Nano Materials & Technology, Yunnan University, Kunming 650091, China*
[4]*zhangch@mail.ustc.edu.cn*
[5]*wenxu_issp@aliyun.com*

Abstract: We present an optical investigation on $La_{0.33}Pr_{0.34}Ca_{0.33}MnO_3$ (LPCMO) nanowires by using standard near-infrared (NIR) reflection experiments. It is found that the samples can respond strongly to the NIR radiation so that the temperature dependence of the reflectivity can be measured accordingly. Interestingly, the temperature induced phase separation and nano-droplet states in the nanowire samples with different diameters can be identified and observed optically without making ohmic contact electrodes on the samples. The onset temperature of the nano-droplet state measured optically is in line with that obtained from previous transport measurements. Importantly, via examining the dependence of the NIR reflectivity upon radiation wavelength, we find that the electronic localization effect exists in the LPCMO nanowires in both electronic states. Such information cannot be directly obtained from electric transport and magneto-transport experiments. The interesting and important experimental findings from this study demonstrate that the simple and contactless NIR reflection measurements can be employed to conveniently study and characterize the basic physical properties of perovskite manganites based nanostructure systems.

OCIS codes: (120.1880) Detection; (160.4236) Nanomaterials; (120.5700) Reflection; (310.6860) Thin films, optical properties; (070.4790) Spectrum analysis.

References and links

1. M. Law, J. Goldberger, and P. D. Yang, "Semiconductor nanowires and nanotubes," Annu. Rev. Mater. Res. **34**, 83–122 (2004).
2. W. Lu and C. M. Lieber, "Semiconductor nanowires," J. Phys. D: Appl. Phys. **39**(21), R387–R406 (2006).
3. Y. Li, F. Qian, J. Xiang, and C. M. Lieber, "Nanowire electronic and optoelectronic devices," Mater. Today **9**(10), 18–27 (2006).
4. X. Y. Ma, H. Zhang, J. Xu, J. J. Niu, Q. Yang, J. Sha, and D. R. Yang, "Synthesis of $La_{1-x}Ca_xMnO_3$ nanowires by a sol–gel process," Chem. Phys. Lett. **363**(5–6), 579–582 (2002).
5. T. V. A. Nguyen, A. N. Hattori, M. Nagai, T. Nakamura, M. Ashida, and H. Tanaka, "Electrical transport properties of (La,Pr,Ca)MnO_3 nanowires investigated using terahertz time domain spectroscopy," J. Appl. Phys. **119**(12), 125102 (2016).
6. A. N. Hattori, Y. Fujiwara, K. Fujiwara, T. V. A. Nguyen, T. Nakamura, M. Ichimiya, M. Ashida, and H. Tanaka, "Identification of giant mott phase transition of single electric nanodomain in manganite nanowall wire," Nano Lett. **15**(7), 4322–4328 (2015).
7. A. P. Ramirez, "Colossal magnetoresistance," J. Phys.: Condens. Matter **9**(39), 8171–8199 (1997).
8. H. Y. Zhai, J. X. Ma, D. T. Gillaspie, X. G. Zhang, T. Z. Ward, E. W. Plummer, and J. Shen, "Giant discrete steps in metal-insulator transition in perovskite manganite wires," Phys. Rev. Lett. **97**(16), 167201 (2006).
9. T. Z. Ward, S. Liang, K. Fuchigami, L. F. Yin, E. Dagotto, E. W. Plummer, and J. Shen, "Reemergent metal-insulator transitions in manganites exposed with spatial confinement," Phys. Rev. Lett. **100**(24), 247204 (2008).

#302344 https://doi.org/10.1364/OME.7.003809
Journal © 2017 Received 12 Jul 2017; revised 26 Sep 2017; accepted 26 Sep 2017; published 2 Oct 2017

Optical Materials EXPRESS

10. G. Singh-Bhalla, S. Selcuk, T. Dhakal, A. Biswas, and A. F. Hebard, "Intrinsic tunneling in phase separated manganites," Phys. Rev. Lett. **102**(7), 077205 (2009).
11. K. X. Zhang, L. Li, H. Li, Q. Y. Feng, N. Zhang, L. Cheng, X. D. Fan, Y. B. Hou, Q. Y. Lu, Z. Y. Zhang, and C. G. Zeng, "Quantum percolation and magnetic nanodroplet states in electronically phase-separated manganite nanowires," Nano Lett. **17**(3), 1461–1466 (2017).
12. C. Zhang, F. H. Su, J. M. Dai, L. Pi, H. Y. Mei, P. Zhang, and W. Xu, "Characterization of material parameters of $La_{0.33}Pr_{0.34}Ca_{0.33}MnO_3$ thin film by terahertz time-domain spectroscopy," Jpn. J. Appl. Phys. **55**(3), 031101 (2016).
13. X. Q. Zou, J. S. Luo, D. W. Lee, C. W. Cheng, D. Springer, S. K. Nair, S. A. Cheong, H. J. Fan, and E. E. M. Chia, "Temperature-dependent terahertz conductivity of tin oxide nanowire films," J. Phys. D: Appl. Phys. **45**(46), 465101 (2012).
14. T. L. Cocker, L. V. Titova, S. Fourmaux, H. C. Bandulet, D. Brassard, J. C. Kieffer, M. A. El Khakani, and F. A. Hegmann, "Terahertz conductivity of the metal-insulator transition in a nanogranular VO_2 film," Appl. Phys. Lett. **97**(22), 221905 (2010).
15. J. R. Simpson, H. D. Drew, V. N. Smolyaninova, R. L. Greene, M. C. Robson, A. Biswas, and M. Rajeswari, "Temperature-dependent scattering rate and optical mass of ferromagnetic metallic manganites," Phys. Rev. B **60**(24), R16263–R16266 (1999).
16. L. Li, H. Li, X. F. Zhai, and C. G. Zeng, "Fabrication and magnetic properties of single-crystalline $La_{0.33}Pr_{0.34}Ca_{0.33}MnO_3$/MgO nanowires," Appl. Phys. Lett. **103**(11), 113101 (2013).
17. N. V. Smith, "Classical generalization of the Drude formula for the optical conductivity," Phys. Rev. B **64**(15), 155106 (2001).

1. Introduction

With the development of nanoscience and nanotechnology, nowadays it has become possible to realize different nanowire (NW) and NW array systems on the basis of electronic materials such as metals, semiconductors, oxides, etc [1]. These NW systems possess many unique and interesting physical properties in contrast to the bulk and thin film samples [2] and can be applied for advanced electronic, optic, and optoelectronic devices [3]. At present, the investigation and characterization of different NW structures have become an important and fast-growing field of research in condensed matter physics, electronics and material science. In particular, the perovskite manganites based NW systems, such as $La_{1-x}Ca_xMnO_3$ NWs, have received a great attention due to their potential applications in electronic and magneto-electronic devices [4–6]. Since the physical properties of the perovskite manganite systems are governed by complex interactions between charge, lattice, orbital, and spin degrees of freedom, a variety of unusual effects, such as colossal magneto-resistance, temperature induced metal-insulator transition, and electronic phase separation have been observed and investigated [7–10].

Recently, high quality and edge-free $La_{0.33}Pr_{0.34}Ca_{0.33}MnO_3$/MgO core-shell NWs were fabricated and the corresponding electronic transport and magneto-transport measurements were performed to study the properties of temperature and magnetic field induced phase separation in such NW systems [11]. It has been found that: i) at relatively low temperatures, the LPCMO NW is in a quantum percolation state (QPS) which is dominated by the ferromagnetic metallic (FMM) phase; ii) at intermediate temperatures, the NW is in a phase separation state (PSS) in which the FMM phase and insulating phases coexist. The critical temperature between the QPS and PSS is about 65 K at B = 0; and iii) at relatively high temperatures, the LPCMO NW is dominated by the insulating phases, but with magnetic nano-droplet state (NDS) emerging at about 200 K [11].

It should be noticed that due to technical difficulties, it is usually very hard to make ohmic contact electrodes on a single NW [11]. As a contactless measurement technique, the optical experiments can be conveniently employed to measure the physical properties of the perovskite manganite NWs. Very recently, we have studied the optical conductivity of LPCMO thin films using terahertz (THz) time-domain spectroscopy (TDS) [12]. By fitting the real and imaginary parts of the optical conductivity obtained experimentally with theoretical formula, the important sample and material parameters such as the electronic relaxation time and carrier density can be determined optically [13,14]. It is found that different electronic states usually correspond to different values of the optical conductivity

Optical Materials EXPRESS

[5,15], and the competitions between them can strongly affect the overall optical properties of these materials [12]. However, the THz-TDS technique requires expensive facilities such as femtosecond laser sources and is mainly based on optical transmission measurement. In this study, we examine the optical properties of $La_{0.33}Pr_{0.34}Ca_{0.33}MnO_3$ core-shell NW systems via measuring the dependence of the NIR reflection spectra upon temperature and radiation wavelength for samples with different wire diameters. The prime motivation of this study is to apply the simple and standard optical experiment for the characterization and investigation of LPCMO NWs.

2. Results and discussion

The LPCMO/MgO core-shell NWs samples are grown via a two-step approach reported in previous study [11,16] including: i) the vapor-liquid-solid growth of the core MgO NWs on MgO substrate using chemical vapor deposition and ii) the growth of the LPCMO shell layers through pulse laser deposition. The diameter of the as-grown MgO cores is about 20 nm and the thickness of the LPCMO shells can be easily controlled via varying the depositing time. Figure 1(b) shows the SEM image of the LPCMO NW sample and Fig. 1(c) shows the statistical distribution of the diameters of the nanowires. The mean diameter of these nanowires is evaluated to be 22.7 nm with a standard deviation of 4.3 nm. In the present study, the mean diameters of the corresponding LPCMO NW samples are 22.7 nm and 44.3 nm (standard deviation is 10.8 nm) respectively, while the length of the NWs is about 1-10 μm. It should be noted that the LPCMO NWs are randomly distributed on the substrate without specific spatial orientation. Therefore, the results obtained from optical measurement are statistical since the focused spot of the NIR light beam is much larger than the diameter of the NWs.

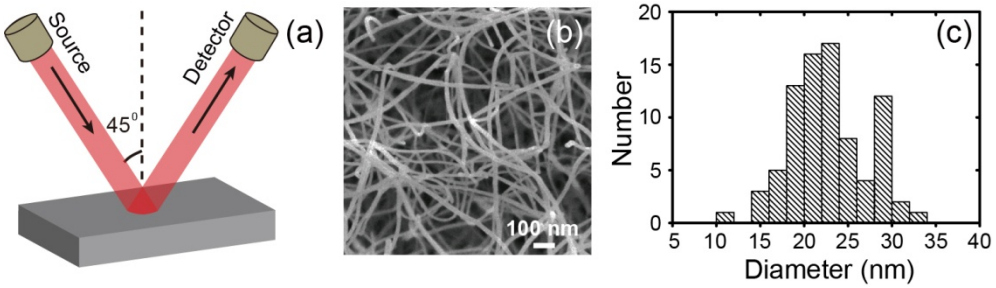

Fig. 1. (a) Schematic diagram of the near-infrared optical reflection measurement for LPCMO NW samples. Here, the incident and emergent light beams are setting at 45° angle to the sample surface. (b) SEM image of LPCMO NW sample with a mean diameter of 22.7 nm. (c) Statistical distribution of LPCMO NW diameters.

The optical reflection (OR) measurements are carried out in the NIR bandwidth (1.4-1.8 μm in wavelength). The standard deuterium lamp is employed as broadband incident NIR light source. In the experiments, the incident and emergent light beams are setting at 45° angle to the sample surface as shown in Fig. 1(a). In this configuration, the incident light field can couple with the electrons in the LPCMO NWs and the OR spectrum can carry the information about how electrons in the sample respond to the applied radiation field. The OR spectrum is recorded using an imaging spectrometer (iHR320 HORIBA Jobin Yvon Inc., Edison, NJ, USA), where the InGaAs photodetector is used for the detection of the NIR light beams in 1.4-1.8 μm wavelength regime. In the experiments, NIR reflection from gold mirror is applied as reference. We measure the reflection spectra for the LPCMO NWs and the reference gold mirror from 10 K to 280 K, where the variation of temperature is achieved in a liquid-helium cooling system (Oxford, UK). The NIR reflection spectra for MgO substrate were measured at corresponding temperatures. We find that the NIR reflectivity of the MgO substrate is little (< 1%) from 10 K to 120 K and is rather weak from 120 K to 280 K (< 5%).

Optical Materials EXPRESS

These values are much smaller than those obtained for the whole sample (i.e., NW layer plus substrate). Together the fact that the incident NIR light beams first irradiate on the NW layer then transmit on the substrate after reflection and absorption from the NW layer, the reflection of the light beams from the MgO layer affects very weakly on the reflection spectra of the whole sample. As a result, the reflection signals of the samples, shown in Fig. 3(a) and Fig. 3(b), come mainly from the LPCMO shell layers.

When an optoelectronic system is subjected to a radiation field, the optical absorption, reflection, and transmission occur simultaneously. The optical absorptance A, the reflectivity R, and the light transmittance T should satisfy: $A + R + T = 1$, required by the energy conservation law. In principle, the optical absorptance is proportional to the optical conductivity $\sigma(\omega) = \sigma_1(\omega) + i\sigma_2(\omega)$ and the optical transmittance is inversely proportional to the optical conductivity $\sigma(\omega)$. Here ω is the radiation frequency. Furthermore, $\sigma(\omega)$ is proportional to $1/\rho$ with ρ being the DC resistivity of a sample. As a result, the NIR reflectivity measured here can reflect the features of DC conductivity or resistivity for a LPCMO NW sample in different electronic states.

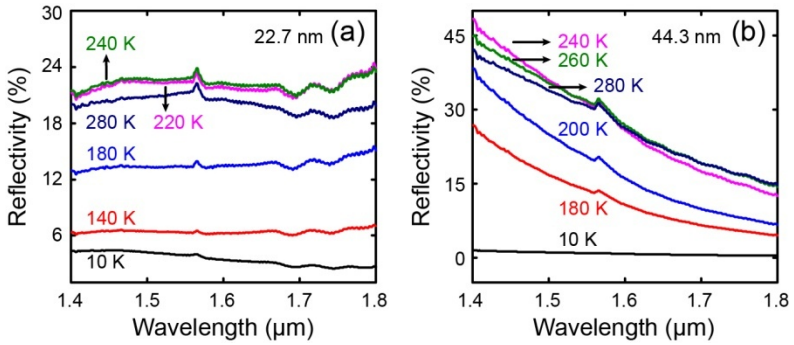

Fig. 2. The spectra of optical reflectivity for LPCMO NW samples with 22.7 nm in (a) and 44.3 nm in (b) wire diameters at different temperatures. The small peak at about 1566 nm is one of the characteristic lines of the deuterium lamp.

The NIR reflection spectra for LPCMO NW samples with the diameter of 22.7 nm and 44.3 nm measured at different temperatures are shown respectively in Fig. 2 (a) and 2(b). As we can see, in 1.4-1.8 μm wavelength regime the intensity of NIR reflection for both samples depends strongly on the temperature over 10 K to 280 K. We note that in Fig. 2 the small peak at about 1566 nm is one of the characteristic lines of the deuterium lamp. To give a clearer view, the optical reflectivity as a function of temperature at different radiation wavelength is shown in Fig. 3. We find that: i) the NIR reflectivity first increases then decreases with increasing temperature for both samples. The peak temperature shifts slightly with varying the radiation wavelength; ii) for the sample with a NW diameter of 44.3 nm, the reflectivity increases monotonously with decreasing radiation wavelength over 10 K to 280 K temperature regime, whereas for the sample with a NW diameter of 22.7 nm the effect of the radiation wavelength at a given temperature is relatively weak; iii) the sample with a NW diameter of 44.3 nm reflects the NIR radiation more strongly than that with a diameter of 22.7 nm (see insert in Fig. 3(a)); and iv) a notable drop of the reflectivity can be observed around 200 K over radiation wavelength from 1.4 μm to 1.8 μm.

In LPCMO NW systems, the metallic and insulating phases coexist and their ratio varies markedly with varying temperature. For LPCMO NWs, the observed resistance kink at T^* (~200 K) is mainly attributed to the onset of the magnetic NDS [11]. The nanoscale droplet with short-range ferromagnetic interaction emerges at about 200 K and it is the precursor of the FMM phase. With decreasing temperature, the magnetic NDS grows in size and eventually stabilizes the FMM phase with long-range order. When temperature is below T^*, the DC resistance of the sample increases with decreasing temperature so that the NIR

Optical Materials EXPRESS

reflectivity decreases with decreasing temperature as shown in Fig. 3. A notable variation of the NIR reflectivity at about 200 K should correspond to the critical temperature between PSS and NDS. Figure 3(c) shows the derivative of the temperature dependence of the reflectivity at 1.6 μm for samples with different NW diameters. The onset temperature of the nano-droplet state can be extracted from the Gaussian fitting, which is evaluated to be 179.6 K (195.7 K) with a standard deviation of 2.0 K (2.6 K) for 22.7 nm (44.3 nm) wire diameter sample. At relatively low-temperatures LPCMO NWs are in the QPS and PSS which have relatively large DC resistance [11]. As a result, the NIR reflectivity is relatively weak at low-temperatures.

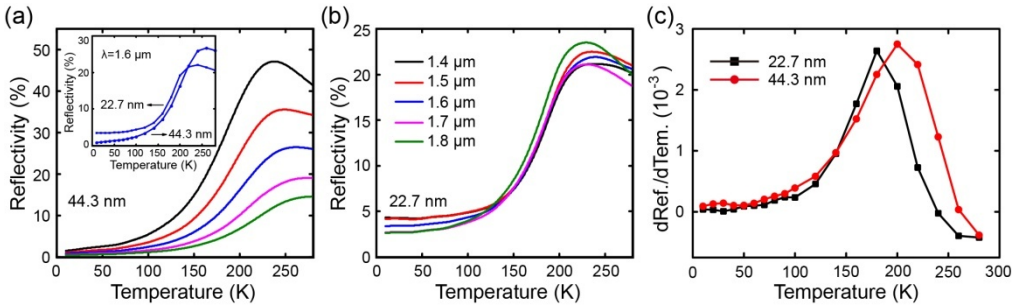

Fig. 3. The reflectivity for LPCMO NWs as a function of temperature for different radiation wavelengths as indicated. The results are shown for wire diameters being 44.3 nm in (a) and 22.7 nm in (b). The insert in (a) shows the results of the reflectivity at 1.6 μm for different wire diameters for comparison. (c) The derivative of the reflectivity at 1.6 μm for different wire diameters.

As we can see from Fig. 3, the NIR reflectivity for LPCMO NW samples increases rather slowly within the temperature range from 10 K to about 100 K, especially for the sample with 22.7 nm wire diameter. This is because the LPCMO NWs are mainly in the stability FMM phase at low temperatures [11]. In the temperature regime from ~100 K to ~240 K for 22.7 nm wire diameter sample and to ~260 K for 44.3 nm wire diameter sample, the magnetic nano-droplets grow in size when temperature decreases. Consequently, the NIR reflectivity increases rapidly with increasing temperature. When temperature is above ~240 K for 22.7 nm wire diameter sample and is above ~260 K for 44.3 nm wire diameter sample, the NIR reflectivity decreases slightly with increasing temperature for LPCMO NW samples. This is induced by the magnetic NDS. We note that by applying the NIR reflection experiment, we cannot observe the critical temperature (~65 K) between the QPS and PSS which is measured by electronic transport experiment [11]. The main reason behind this is that the fraction of the insulating phases change a little at about 65 K and it cannot be obviously seen by the NIR reflection experiments. At about 65 K, there is a very small fraction of the insulating domains which act as the tunneling barriers. As indicated in Ref [11], such remnant insulating domains are quite robust, and cannot convert to metallic domains even under low temperature and high magnetic field up to 14 T.

It can be seen from Fig. 3 that the NIR reflectivity of the LPCMO NWs decreases with increasing radiation wavelength, especially for the sample with 44.3 nm wire diameter. This effect can be more clearly observed at relative high temperatures. As we know, the optical conductivity for free electrons in metallic states can be described by the Drude formula which suggests that the real part of the optical conductivity should decrease monotonically with increasing radiation frequency ω, namely the standard Drude formula can result in an effect that the optical reflectivity increases with increasing radiation wavelength, which is contradictory to our experimental findings. In 2001, Smith developed a modified Drude formula in which the light field induced backscattering or electronic localization effect has been taken into consideration. In such a case, the complex optical conductivity in an electronic system can be described as [17]

Optical Materials EXPRESS

$$\sigma(\omega) = \frac{\sigma_0}{1 - i\omega\tau}[1 + \sum_{n=1}^{\infty} \frac{c_n}{(1 - i\omega\tau)^n}] \quad (1)$$

Here the DC conductivity σ_0 is given by $N_e e^2\tau/m^*$ with the carrier density N_e, the momentum relaxation time τ, and the electron effective mass m^*. Moreover, the coefficient c_n is a parameter describing the fraction of original velocity for an electron after n^{th} scattering events. For $c_n = 0$, Eq. (1) becomes the standard Drude formula. For a nonzero c_n or in the presence of electronic localization effect, the optical conductivity can increase with ω [17]. The experimental results shown in Fig. 3 suggest that the electronic localization effect is present in LPCMO NWs. The increase in the reflectivity with NIR wavelength can be more markedly observed at relatively higher temperatures when the localization effect is stronger in LPCMO NWs. Thus, we are able to understand the dependence of NIR reflectivity on radiation wavelength and temperature for LPCMO NWs with the help of DC resistivity obtained experimentally and the Drude-Smith formula developed theoretically. We notice that the NIR reflectivity for a sample with 22.7 nm NW diameter has relatively weak dependence on radiation wavelength. In LPCMO NW samples, the magnetic nano-droplet phase and the ferromagnetic metallic phase serve as the metallic (or conducting) domain in neighboring insulate phases, and the size of the metallic domain is comparable to the lateral size [11]. The LPCMO NW sample with a larger diameter has a higher electric conductivity, which is attributed to the increase in metallic domain-to-domain contact junctions and to the long diffusion length of the carriers through the metallic domain network. As a result, the sample with 22.7 nm wire diameter has relatively larger resistivity (i.e., with a smaller electronic relaxation time τ and a smaller value of $\omega\tau$) so that the optical effect is relatively weak for this sample in the NIR bandwidth.

3. Conclusion

In summary, by employing the standard NIR reflection experiments, we are able to conveniently study and characterize the NIR optical properties of LPCMO NW systems without making ohmic contact electrodes achieved by using sophisticated nanofabrication techniques. Through examining the temperature dependence of the optical reflectivity, we can detect optically the temperature dependence of phase transition in these samples. The results obtained from this study have shown that the temperature induced phase transition in LPCMO NW systems can be detected optically via NIR reflection experiments. Through examining the dependence of the optical reflectivity on radiation wavelength, we are able to detect the effect of electronic localization in these sample systems. Such information cannot be obtained directly from conventional electric transport measurements. We hope the results obtained from this work and discussed here can help us to gain an in-depth understanding of the physical properties of the newly developed perovskite manganite based nanostructure systems and to provide a simple experimental technique for the investigation and characterization of these nanostructure systems.

Funding

National Natural Science Foundation of China (11574319, 11304317, 11304272); Ministry of Science and Technology of China (2011YQ130018); and the Department of Science and Technology of Yunnan Province (2013FD003).

Acknowledgments

We would like to thank Dr. L. Li and associates at the University of Science and Technology of China for providing the $La_{0.33}Pr_{0.34}Ca_{0.33}MnO_3$ nanowire samples for this study.